Molecular Pharmacology Fast Forward. Published on July 24, 2017 as DOI: 10.1124/mol.117.109199
This article has not been copyedited and formatted. The final version may differ from this version.

Splice variants of pH-sensitive chloride channel identify a key determinant of ivermectin sensitivity in the larvae of the silkworm *Bombyx mori*

Daiki Okuhara, Shogo Furutani, Katsuhiko Ito, Makoto Ihara and

Kazuhiko Matsuda

Department of Applied Biological Chemistry, Faculty of Agriculture, Kindai University, 3327-204 Nakamachi, Nara 631-8505, Japan (DO, SF, MI, KM)

Tokyo University of Agriculture and Technology, 3-5-8 Saiwai-cho, Fuchu City, Tokyo 183-8509, Japan (KI)

Primary Laboratory Origin

Department of Applied Biological Chemistry, Faculty of Agriculture, Kindai University

Molecular Pharmacology Fast Forward. Published on July 24, 2017 as DOI: 10.1124/mol.117.109199
This article has not been copyedited and formatted. The final version may differ from this version.

Running title: Determinant of ivermectin action on pHCl

To whom correspondence should be addressed: Kazuhiko Matsuda

Department of Applied Biological Chemistry, Faculty of Agriculture, Kinki University

3327-204 Nakamachi, Nara 631-8505, Japan

Tel. +81-742-437153; Fax: +81-742-431445; E-mail:

kmatsuda@nara.kindai.ac.jp

Number of text pages	34
Number of tables	1
Number of supplementary tables	2
Number of figures	6
Number of references	41
Number of words in Abstract	243 words
Number of words in Introduction	519 words
Number of words in Discussion	566 words

Abbreviations: HEPES, 4-(2-hydroxyethyl)piperazine-1-ethanesulfonic acid; SOS, standard oocyte saline

Molecular Pharmacology Fast Forward. Published on July 24, 2017 as DOI: 10.1124/mol.117.109199
This article has not been copyedited and formatted. The final version may differ from this version.

Abstract

The pH-sensitive chloride channels (pHCls) are broadly expressed in insects, but little is known about their physiological role, diversity and sensitivity to insecticides acting on relevant chloride channels. Here we have sequenced 50 transcripts of the pHCl-1 gene from the brain, third thoracic ganglion (T3G) and midgut of larvae of silkworm *Bombyx mori*. It was found that >50 variants were expressed with distinct splicing in the T3G compared to the brain and midgut. Of the variants detected, variant 9, which was expressed most abundantly in the larvae, was reconstituted in *Xenopus laevis* oocytes to characterise its pH- and ivermectin sensitivity. Variant 9 formed a functional pHCl with half-maximal activation at a pH of 7.87, and was activated by ivermectin irrespective of the extracellular pH. This was in contrast to variant 1, which was activated more profoundly at acidic rather than basic pH. To identify a key determinant for such differential ivermectin sensitivity, different amino acids in variants 1 and 9 were swapped, and the effects of the mutations on ivermectin sensitivity were investigated. The V275S mutation of variant 1 enhanced ivermectin sensitivity, whereas the S275V mutation of variant 9 caused a reduction in sensitivity. In homology models of the *Bombyx* pHCls, Val275 of variant 1 interacted more

Molecular Pharmacology Fast Forward. Published on July 24, 2017 as DOI: 10.1124/mol.117.109199
This article has not been copyedited and formatted. The final version may differ from this version.

strongly with Ala273 than Ser275 of variant 9 at the channel gate. This interaction is likely to prevent ivermectin-induced opening of the channel, accounting, at least partially, for the differential macrolide action on the two variants.

Molecular Pharmacology Fast Forward. Published on July 24, 2017 as DOI: 10.1124/mol.117.109199
This article has not been copyedited and formatted. The final version may differ from this version.

Introduction

Most commercial pesticides modulate neural transmission and thus exhibit rapid toxicity to pests. One major pesticide target is the pentameric ligand-gated ion channels (pLGICs) (Nemecz et al., 2016; Sine and Engel, 2006) that mediate fast-acting neural transmission in insects. For example, neonicotinoids (Matsuda et al., 2001; Matsuda et al., 2009; Matsuda et al., 2005; Thany et al., 2007; Tomizawa and Casida, 2003; Tomizawa and Casida, 2005), flupyradifurone (Jeschke et al., 2013; Nauen et al., 2015), sulfoxaflor (Sparks et al., 2013) and triflumezopyrim (Cordova et al., 2016; Zhang et al., 2017) modulate nicotinic acetylcholine receptors (nAChRs), while fipronil (Ikeda et al., 2004; Ikeda et al., 2001) and broflanilide (Nakao and Banba, 2015; Nakao and Banba, 2016) selectively block γ-aminobutyric acid receptors (GABARs). The pLGICs open an integrated ion channel in response to agonist binding at the orthosteric site. Each subunit possesses an extracellular N-terminal region containing a cysteine loop and four transmembrane (TM) domains in which TM2 forms the channel lining (Nemecz et al., 2016; Sine and Engel, 2006).

While nAChRs and GABARs play a central role in neural transmission in vertebrates and invertebrates, glutamate-gated chloride channels (GluCls)

Molecular Pharmacology Fast Forward. Published on July 24, 2017 as DOI: 10.1124/mol.117.109199
This article has not been copyedited and formatted. The final version may differ from this version.

(Wolstenholme, 2012), histamine-gated chloride channels (HisCls) (Gisselmann et al., 2002; Hardie, 1989; Zheng et al., 2002) and pH-sensitive chloride channels (pHCls) (Mounsey et al., 2007; Nakatani et al., 2016; Schnizler et al., 2005) are expressed only in the invertebrate nervous system to maintain homeostasis. Such invertebrate-specific channels are important targets of safer insecticides (Bloomquist, 2003; Raymond and Sattelle, 2002), and indeed, a macrocyclic compound ivermectin that primarily modulates GluCl (Cully et al., 1994), is used worldwide as an antihelmintic and pesticide (Wolstenholme, 2012). In contrast to GluCls and HisCls, the role of the pHCl, which now should be referred to as pHCl-1, in physiology is largely unknown because its native ligand has not been identified. The pHCl-1 is expressed in the central nervous system and hindgut, and forms chloride channels in *Drosophila*, and its chloride channel is opened in response to shifts in extracellular pH (Schnizler et al., 2005). Recently, a second pHCl, pHCl-2, has been discovered; it is expressed in *Drosophila* Malpighian tubules to control fluid secretion (Feingold et al., 2016).

Of the pHCl-1 variants found in *Drosophila*, variant A was described as being activated by ivermectin at acidic as well as basic pH (Schnizler et al., 2005), whereas the *Bombyx* variant A was activated by ivermectin more

Molecular Pharmacology Fast Forward. Published on July 24, 2017 as DOI: 10.1124/mol.117.109199
This article has not been copyedited and formatted. The final version may differ from this version.

profoundly at acidic rather than basic pH (Nakatani et al., 2016). This raises the following questions: 1) whether the pH-dependent ivermectin sensitivity of the pHCl-1 is found in all variants in *Bombyx*; and 2) what structural feature underpins the differences between the *Drosophila* and *Bombyx* pHCl-1 variants.

The aim of this study was to clarify how the pHCl-1 gene transcript diverges in *Bombyx* and whether all of the variants exhibit similar ivermectin sensitivity. We isolated and sequenced 50 pHCl gene transcripts from the brain, T3G and midgut of *Bombyx* larvae, to characterise a major variant in terms of the response to pH shifts and ivermectin sensitivity. In addition, we mutated variants 1 and 9 to elucidate a determinant of the differential ivermectin action.

Materials and methods

Chemicals

22,23-Dihydroavermectin B1a (Ivermectin), penicillin, streptomycin and sodium pyruvate were purchased from Sigma-Aldrich (St. Louis, Missouri, USA), while 4-(2-hydroxyethyl)-1-piperazineethanesulfonic acid (HEPES), gentamycin, NaCl and KCl were purchased from Nacalai Tesque (Kyoto, Japan). $CaCl_2$ and $MgCl_2$ were purchased from Wako Pure Chemical Industries (Osaka, Japan).

Molecular Pharmacology Fast Forward. Published on July 24, 2017 as DOI: 10.1124/mol.117.109199
This article has not been copyedited and formatted. The final version may differ from this version.

Cloning of pHCl cDNAs from silkworm larvae

Total RNA was extracted from the brain, third thoracic ganglion (T3G) and midgut of silkworm larvae (p50 strain) using TRIzol reagent (Thermo Fisher Scientific, Waltham, MA USA), and mRNA was purified using TURBO DNase (Thermo Fisher Scientific). To generate silkworm larva cDNA, a reverse transcription reaction was performed using PrimeScript™ RT Reagent Kit (Takara Bio, Shiga, Japan). First-round PCR of full-length cDNA was amplified with the KOD -Plus- DNA polymerase (Toyobo, Osaka, Japan) using pHCl_Forward_1 (Forward: GAGTGCTGAAGACAGCAAACGCGA) and pHCl_Reverse_1 (Reverse: ACAGTACCTCCGAATGTCACACCA) primers by 32 cycle reactions of 94°C 15 s, 55°C 30 s and 68°C 2 min. Second-round PCR was performed using KOD -Plus- polymerase with BmpHCl_5 (Forward: CGGGGTACCGCCGCCATGGGTTGGTCATGCGTCG) and BmpHCl_3 (Reverse: CCGCTCGAGTTAAGAAAACGCTTTGTAGTGAATG) primers by 32 cycle reactions of 94°C 15 s, 58°C 30 s and 68°C 2 min. DNA bands were purified by agarose gel electrophoresis and cloned into the TOPO vector (Thermo Fisher Scientific) for automated sequencing using the 3130xl Genetic Analyzer (Thermo Fisher Scientific).

Molecular Pharmacology Fast Forward. Published on July 24, 2017 as DOI: 10.1124/mol.117.109199
This article has not been copyedited and formatted. The final version may differ from this version.

When pHCl variants were expressed in *Xenopus laevis* oocytes, cDNAs were cloned into the pcDNA 3.1 (+) vector (Thermo Fisher Scientific) and each cRNA was prepared as described in the next section. cDNAs were mutated by PCR with PrimeSTAR Max DNA Polymerase (Takara Bio) using forward and reverse primers (Supplementary Table 1) by 10 cycle reactions of 98°C 10 s, 55°C 5 s and 72°C 2 min, followed by DpnI digestion to remove templates. *Escherichia coli* was then transformed with the PCR product to obtain mutated plasmid DNAs. All mutant cDNAs were sequenced to confirm their structures.

Preparation of cRNAs

The pcDNA 3.1 (+) vector harbouring the BmpHCl cDNAs was digested by XhoI and cRNA was transcribed from the linearized vector using a mMESSAGE mMACHINE T7 Ultra Kit (Thermo Fisher Scientific). cRNA solutions were dissolved in RNase-free water at 1 mg/ml and stored at −80°C before use.

Two-dimensional clustering analysis

Two-dimensional (2D) hierarchical clustering was conducted to identify coordinated networks in exon selection. The Z scores of the sequence detection

Molecular Pharmacology Fast Forward. Published on July 24, 2017 as DOI: 10.1124/mol.117.109199
This article has not been copyedited and formatted. The final version may differ from this version.

abundance were correlated with the three tissues, and illustrated by R software (R Core Team, R Foundation for Statistical Computing, Vienna, Austria, 2015).

Expression of Bombyx pHCls in Xenopus oocytes

Ovaries were excised from anaesthetized female *X. laevis* as previously described, in accordance with the U.K. Animals (Scientific Procedures) Act, 1986 (Ihara et al., 2003; Matsuda et al., 1998; Nakatani et al., 2016; Shimomura et al., 2002; Shimomura et al., 2006). The oocytes were treated with collagenase (Type IA, Sigma-Aldrich) in Ca^{2+}-free standard oocyte saline (Ca^{2+}-free SOS) with the following composition (mM): NaCl 100, KCl 2.0, $MgCl_2$ 1.0 and 4-(2-hydroxyethyl)-1-piperazineethanesulfonic acid (HEPES) 5.0 (pH 7.6). Oocytes were then transferred to SOS containing 100 mM NaCl, 2 mM KCl, 1 mM $MgCl_2$, 1.8 mM $CaCl_2$ and 5 mM HEPES (pH 7.6) to remove follicle membranes, and were injected with 50 nl of cRNA solution. cRNA-injected oocytes were incubated for four days in SOS supplemented with penicillin (100 units ml^{-1}), streptomycin (100 μg ml^{-1}), gentamycin (20 μg ml^{-1}) and sodium pyruvate (2.5 mM) prior to electrophysiological experiments.

Molecular Pharmacology Fast Forward. Published on July 24, 2017 as DOI: 10.1124/mol.117.109199
This article has not been copyedited and formatted. The final version may differ from this version.

Voltage-Clamp Electrophysiology

Two-electrode voltage-clamp electrophysiology was performed as previously described (Ihara et al., 2003; Matsuda et al., 1998; Nakatani et al., 2016; Shimomura et al., 2002; Shimomura et al., 2006). Oocytes were perfused with the SOS. The voltage-clamp set-up was established using a GeneClamp 500B amplifier (Molecular Devices, Sunnyvale, California, USA) at a holding potential of −80 mV, and membrane currents induced in response to a pH shift or ivermectin were recorded using Clampex 8 software (Molecular Devices). The current data were digitized by a Digidata 1200 A/D converter (Molecular Devices) and analyzed using Clampfit 9 software (Molecular Devices).

Data analysis

The reversal potential for the pH shift-induced response of pHCl was determined by normalising the peak current response at each membrane potential by that measured at −100 mV and then drawing the normalized peak current amplitude–membrane potential relationship. The reversal potential was determined not only in normal SOS (Cl: 107.6 mM), but also in low-chloride SOS (Cl: 37.6 mM) where some of the NaCl was substituted with Na isethionate.

Molecular Pharmacology Fast Forward. Published on July 24, 2017 as DOI: 10.1124/mol.117.109199
This article has not been copyedited and formatted. The final version may differ from this version.

The peak current amplitude of each response to the pH shift from pH 6.0 was normalized by the peak current amplitude of the response induced by the shift to pH 9.0, while the peak amplitude of each response to various concentrations of ivermectin was normalized by the peak amplitude of the response to 10 μM ivermectin. Each data was obtained as mean ± standard deviation of the mean (n = 4 or 5 oocytes from two female frogs). The normalized response was fitted by non-linear regression using Prism software version 6.05 (GraphPad, La Jolla, California, USA), according to the following equation where Y is the normalized response, Imax is the normalized maximum response, pH_{50} is the pH giving the half-maximal response and n_H is the Hill coefficient:

$$Y = \frac{I_{max}}{1 + 10^{(\log pH_{50} - [A])nH}}.$$

Drug application

Ivermectin was stored as a 100 mM dimethyl sulfoxide (DMSO) stock solution at −20°C until use, and the stock solution was diluted with SOS to prepare test solutions. Ivermectin was applied in SOS to oocytes expressing the *Bombyx* pHCls by increasing the concentration up to 1 μM, but tested on different oocytes at higher concentrations to prevent from irreversible effects.

Molecular Pharmacology Fast Forward. Published on July 24, 2017 as DOI: 10.1124/mol.117.109199
This article has not been copyedited and formatted. The final version may differ from this version.

Homology modelling of pHCls

Homology models of the pHCl variants were constructed using MODELLER (Webb and Sali, 2014). To build the models, the amino acid sequences of pHCl were aligned with those of *Caenorhabditis elegans* GluCl α (PDB: 3RHW) (Hibbs and Gouaux, 2011) when unaligned amino acids in the TM3–TM4 linker were omitted. Bound ivermectin was treated as bulk residues. The models were visualized using PyMOL software (Schrödinger, New York, USA).

Molecular Pharmacology Fast Forward. Published on July 24, 2017 as DOI: 10.1124/mol.117.109199
This article has not been copyedited and formatted. The final version may differ from this version.

Results

Variations of cDNAs of pHCls in Bombyx mori larvae

Full-length cDNAs of the *Bombyx* pHCl gene consisting of 17 exons (Figure 1A) from the brain, 3TG and midgut of the silkworm larvae were amplified by PCR and sequenced. Consequently, 51 variants of the pHCl gene transcripts were found to be generated by alternative splicing at exon 11 as well as partial deletions at exon 15, 16 and 17 (Figure 1B, Supplementary Table 2). Variant A, which is referred to as variant 1 in this study, was detected in the brain, as previously reported (Nakatani et al., 2016). Neither exon 11a, nor 11b, was used to yield some variants (Figure 1B), resulting in a lack of TM1 and part of TM2 (Figure 1B). Variant 9 (Figure 1B) was expressed most abundantly in all three organs investigated. It possessed all of the TM domains, as well as the N-terminus ligand-binding domain, as for variant 1 (Figure 1B).

To understand exon selection tendency in *Bombyx*, 2D clustering analysis was conducted for exons vs tissues. The clustering indicated that exon selection within the T3G was distinct to that seen in the brain and midgut (Figure 2).

Molecular Pharmacology Fast Forward. Published on July 24, 2017 as DOI: 10.1124/mol.117.109199
This article has not been copyedited and formatted. The final version may differ from this version.

Characterisation of variant 9 expressed in Xenopus oocytes

Since variant 9 was expressed most abundantly in *Bombyx*, it was reconstituted in *Xenopus* oocytes and characterized in terms of its functionality as a pHCl and difference in nature from variant 1. In response to extracellular pH shifts from pH 7.6 to 9.0, inward currents were induced in *Xenopus* oocytes expressing variant 9 (Figure 3A). The reversal potential for the peak current amplitude of variant 9 at an extracellular chloride ion concentration of 107.6 mM was −23.7 mV, close to the theoretical equilibrium potential for the chloride ion of −24.9 mV. Reducing the extracellular chloride concentration to 37.6 mM shifted the reversal potential to 1.5 mV, which was also similar to the equilibrium potential of 1.6 mV (Figure 3B).

The peak current amplitude of the pHCl response was enhanced in a pH-dependent manner and was maximal at pH 9.0 (Figure 3C, D). The pH giving a half-maximal response (pH_{50}) was calculated by non-linear regression to be 7.87 ± 0.27 (n = 4) (Figure 3D). No substantial difference in pH_{50} was observed between variant 1 (Nakatani et al., 2016) and 9.

Molecular Pharmacology Fast Forward. Published on July 24, 2017 as DOI: 10.1124/mol.117.109199
This article has not been copyedited and formatted. The final version may differ from this version.

Actions of ivermectin on variant 9 expressed in Xenopus oocytes

A macrolide compound, ivermectin, activates pHCl as well as GluCls. Thus, the compound was tested on variant 9 at four different pHs. Ivermectin induced inward currents in oocytes expressing variant 9 with a similar EC_{50} at all pHs tested (Figure 4A, B, Table 1), in contrast to its action on variant 1 which was more profound at acidic pHs (Nakatani et al., 2016).

Effects of mutations on ivermectin sensitivity of variants 1 and 9

There are different amino acids between variants 1 and 9 (Figure 5A), of which one, or a combination of these, is likely to underpin differential ivermectin sensitivity. Hence, the different amino acids of variant 1 were mutated to the corresponding amino acid of variant 9 and vice versa, and the effects of this on the action of ivermectin on the mutants expressed in *Xenopus* oocytes were investigated at an extracellular pH of 5.5 and 8.5. At pH 5.5, ivermectin activated not only variant 9, but also variant 1, as reported previously (Nakatani et al., 2016). Hence, no clear impact of site-directed mutagenesis was observed (Supplementary Figure 1). At pH 8.5, however, the V275S mutation of variant 1 enhanced the ivermectin-induced response, while the inverse S275V mutation of

Molecular Pharmacology Fast Forward. Published on July 24, 2017 as DOI: 10.1124/mol.117.109199
This article has not been copyedited and formatted. The final version may differ from this version.

variant 9 reduced it (Figure 5B, C), demonstrating that the residue 275 influences sensitivity to the macrolide at the alkaline pH.

To understand the role of Ser/Val275 in determining ivermectin action, homology models of variants 1 and 9 were constructed (Figure 6). The amino acid at position 275 was located at the channel gate and remote from the ivermectin binding site (Figure 6A). Both Val275 of variant 1 and Ser275 of variant 9 had direct contact with Ala273, but the interaction with Ser275 appeared to be weaker than that with Val275 (Figure 6B).

Molecular Pharmacology Fast Forward. Published on July 24, 2017 as DOI: 10.1124/mol.117.109199
This article has not been copyedited and formatted. The final version may differ from this version.

Discussion

To elucidate diversity of the pHCl1 gene product in *Bombyx*, we sequenced 50 cDNAs of the pHCl-1 gene from each of three organs (the brain, T3G and midgut) of silkworm larvae, and found 51 splice variants. We did not detect any RNA editing, but cannot rule out the possibility that it may be present in other tissues and/or at different developmental stages. A similar diversity of pLGICs was also found with respect to nAChRs (Grauso et al., 2002), GABARs (Jones et al., 2009) and GluCls (Furutani et al., 2014; Kita et al., 2014). Notably, diversity of the *Drosophila* GABA receptor RDL resulting from alternative splicing and RNA editing affects the EC_{50} of GABA (Jones et al., 2009), while the differential splicing-induced variations of GluCl affects receptor density in membranes (Furutani et al., 2014). For the *Bombyx* pHCl, we have found for the first time that splice variants exhibit differential sensitivity to ivermectin.

Of the 51 variants, 24 lacked TM1 and part of TM2, and are presumed to be incapable of forming a chloride channel (Nakatani et al., 2016). Nonetheless, they may work either as dominant negative proteins to impair functionality of the variants with all TM domains, as is the case for the β3 subunit that negatively regulates neuronal nAChRs (Broadbent et al., 2006), or as enhancers to assist

Molecular Pharmacology Fast Forward. Published on July 24, 2017 as DOI: 10.1124/mol.117.109199
This article has not been copyedited and formatted. The final version may differ from this version.

in the assembly of the pHCls containing entire TM1 and TM2. In the future, it is necessary to test these hypotheses as well as to investigate co-localization of the TM1-TM2 containing and lacking variants in a single cell. A distinct exon selection was observed in the T3G compared to the other tissues, which may reflect a role of the ganglion in the control of leg motility.

Variant 9, which was most abundant in the *Bombyx* larvae, possesses four different amino acids from variant 1 that is expressed mainly in the brain (Figure 5A). Variant 9 was activated by ivermectin at all of the pHs tested (Figure 4), while variant 1 is activated at acidic pHs (Figure 5B, C) (Nakatani et al., 2016). Ivermectin interacts with the allosteric site formed by TM1, TM2, TM3 and the TM2–TM3 linker (Collins and Millar, 2010; Hibbs and Gouaux, 2011; McCavera et al., 2009) to activate GluCls. However, forward (variant 1 to variant 9) and reverse (variant 9 to variant 1) mutations identified Val275 of variant 1 and Ser275 of variant 9 as those underpinning the differential action of ivermectin on *Bombyx* pHCl (Figure 5B, C). In the homology models, Val275 of variant 1 had stronger contact with Ala 273 than Ser275 in variant 9 (Figure 6B), thereby preventing ivermectin-induced activation. This explanation seems plausible, but we did not take into consideration any effects of pH on the allosteric site

Molecular Pharmacology Fast Forward. Published on July 24, 2017 as DOI: 10.1124/mol.117.109199
This article has not been copyedited and formatted. The final version may differ from this version.

interactions with ivermectin when modelling the *Bombyx* pHCl. Therefore, it will be necessary in future to investigate the effects of amino acids at position 275 on the flexibility of pHCl at the channel gate, as well as on the ivermectin binding to the allosteric site, using molecular dynamics.

In summary, we have found a high diversity of pHCl gene transcripts in *Bombyx*, and such diversity is responsible for the differential action of ivermectin. In addition, we identified a key determinant of ivermectin sensitivity in the pHCl, providing new insight into its pharmacology. To understand the role of the pHCl in maintaining insect homeostasis, it is critical to identify its native ligand.

Authorship contribution

Participated research design: Okuhara, Ihara and Matsuda

Conducted experiments: Okuhara, Furutani, Ito, Ihara and Matsuda

Performed data analysis: Okuhara, Ihara and Matsuda

Wrote or contributed to the writing of the manuscript: Okuhara, Furutani, Ito, Ihara and Matsuda

Molecular Pharmacology Fast Forward. Published on July 24, 2017 as DOI: 10.1124/mol.117.109199
This article has not been copyedited and formatted. The final version may differ from this version.

References

Bloomquist JR (2003) Chloride channels as tools for developing selective insecticides. *Arch Insect Biochem Physiol* **54**:145-156.

Broadbent S, Groot-Kormelink PJ, Krashia PA, Harkness PC, Millar NS, Beato M and Sivilotti LG (2006) Incorporation of the β3 subunit has a dominant-negative effect on the function of recombinant central-type neuronal nicotinic receptors. *Mol Pharmacol* **70**:1350-1357.

Collins T and Millar NS (2010) Nicotinic acetylcholine receptor transmembrane mutations convert ivermectin from a positive to a negative allosteric modulator. *Mol Pharmacol* **78**:198-204.

Cordova D, Benner EA, Schroeder ME, Holyoke CW, Jr., Zhang W, Pahutski TF, Leighty RM, Vincent DR and Hamm JC (2016) Mode of action of triflumezopyrim: A novel mesoionic insecticide which inhibits the nicotinic acetylcholine receptor. *Insect Biochem Mol Biol* **74**:32-41.

Cully DF, Vassilatis DK, Liu KK, Paress PS, Van der Ploeg LH, Schaeffer JM and Arena JP (1994) Cloning of an avermectin-sensitive glutamate-gated chloride channel from *Caenorhabditis elegans*. *Nature* **371**:707-711.

Feingold D, Starc T, O'Donnell MJ, Nilson L and Dent JA (2016) The orphan pentameric ligand-gated ion channel pHCl-2 is gated by pH and regulates fluid secretion in *Drosophila* Malpighian tubules. *J Exp Biol* **219**:2629-2638.

Furutani S, Ihara M, Nishino Y, Akamatsu M, Jones AK, Sattelle DB and Matsuda K (2014) Exon 3 splicing and mutagenesis identify residues influencing cell surface density of heterologously expressed silkworm (*Bombyx mori*) glutamate-gated chloride channels. *Mol Pharmacol* **86**:686-695.

Gisselmann G, Pusch H, Hovemann BT and Hatt H (2002) Two cDNAs coding for histamine-gated ion channels in *D. melanogaster*. *Nat Neurosci* **5**:11-12.

Grauso M, Reenan RA, Culetto E and Sattelle DB (2002) Novel putative nicotinic acetylcholine receptor subunit genes, Dα5, Dα6 and Dα7, in *Drosophila melanogaster* identify a new and highly conserved target of adenosine deaminase acting on RNA-mediated A-to-I pre-mRNA editing. *Genetics*

Molecular Pharmacology Fast Forward. Published on July 24, 2017 as DOI: 10.1124/mol.117.109199
This article has not been copyedited and formatted. The final version may differ from this version.

160:1519-1533.

Hardie RC (1989) A histamine-activated chloride channel involved in neurotransmission at a photoreceptor synapse. *Nature* **339**:704-706.

Hibbs RE and Gouaux E (2011) Principles of activation and permeation in an anion-selective Cys-loop receptor. *Nature* **474**:54-60.

Ihara M, Matsuda K, Otake M, Kuwamura M, Shimomura M, Komai K, Akamatsu M, Raymond V and Sattelle DB (2003) Diverse actions of neonicotinoids on chicken α7, α4β2 and *Drosophila*-chicken SADβ2 and ALSβ2 hybrid nicotinic acetylcholine receptors expressed in *Xenopus laevis* oocytes. *Neuropharmacology* **45**:133-144.

Ikeda T, Nagata K, Kono Y, Yeh JZ and Narahashi T (2004) Fipronil modulation of $GABA_A$ receptor single-channel currents. *Pest Manag Sci* **60**:487-492.

Ikeda T, Zhao X, Nagata K, Kono Y, Shono T, Yeh JZ and Narahashi T (2001) Fipronil modulation of γ-aminobutyric $acid_A$ receptors in rat dorsal root ganglion neurons. *J Pharmacol Exp Ther* **296**:914-921.

Jeschke P, Nauen R and Beck ME (2013) Nicotinic acetylcholine receptor agonists: a milestone for modern crop protection. *Angew Chem Int Ed Engl* **52**:9464-9485.

Jones AK, Buckingham SD, Papadaki M, Yokota M, Sattelle BM, Matsuda K and Sattelle DB (2009) Splice-variant- and stage-specific RNA editing of the Drosophila GABA receptor modulates agonist potency. *J Neurosci* **29**:4287-4292.

Kita T, Ozoe F and Ozoe Y (2014) Expression pattern and function of alternative splice variants of glutamate-gated chloride channel in the housefly *Musca domestica*. *Insect Biochem Mol Biol* **45**:1-10.

Matsuda K, Buckingham SD, Freeman JC, Squire MD, Baylis HA and Sattelle DB (1998) Effects of the α subunit on imidacloprid sensitivity of recombinant nicotinic acetylcholine receptors. *Br J Pharmacol* **123**:518-524.

Matsuda K, Buckingham SD, Kleier D, Rauh JJ, Grauso M and Sattelle DB (2001) Neonicotinoids: insecticides acting on insect nicotinic acetylcholine receptors. *Trends Pharmacol Sci* **22**:573-580.

Matsuda K, Kanaoka S, Akamatsu M and Sattelle DB (2009) Diverse actions and target-site selectivity of neonicotinoids: structural insights. *Mol Pharmacol* **76**:1-10.

Matsuda K, Shimomura M, Ihara M, Akamatsu M and Sattelle DB (2005) Neonicotinoids show selective and diverse actions on their nicotinic receptor targets: electrophysiology, molecular biology, and receptor modeling studies. *Biosci Biotechnol Biochem* **69**:1442-1452.

McCavera S, Rogers AT, Yates DM, Woods DJ and Wolstenholme AJ (2009) An ivermectin-sensitive glutamate-gated chloride channel from the parasitic nematode Haemonchus contortus. *Mol Pharmacol* **75**:1347-1355.

Mounsey KE, Dent JA, Holt DC, McCarthy J, Currie BJ and Walton SF (2007) Molecular characterisation of a pH-gated chloride channel from Sarcoptes scabiei. *Invert Neurosci* **7**:149-156.

Nakao T and Banba S (2015) Minireview: Mode of action of meta-diamide insecticides. *Pestic Biochem Physiol* **121**:39-46.

Nakao T and Banba S (2016) Broflanilide: A meta-diamide insecticide with a novel mode of action. *Bioorg Med Chem* **24**:372-377.

Nakatani Y, Furutani S, Ihara M and Matsuda K (2016) Ivermectin modulation of pH-sensitive chloride channels in the silkworm larvae of Bombyx mori. *Pestic Biochem Physiol* **126**:1-5.

Nauen R, Jeschke P, Velten R, Beck ME, Ebbinghaus-Kintscher U, Thielert W, Wolfel K, Haas M, Kunz K and Raupach G (2015) Flupyradifurone: a brief profile of a new butenolide insecticide. *Pest Manag Sci* **71**:850-862.

Nemecz A, Prevost MS, Menny A and Corringer PJ (2016) Emerging molecular mechanisms of signal transduction in pentameric ligand-gated ion channels. *Neuron* **90**:452-470.

Molecular Pharmacology Fast Forward. Published on July 24, 2017 as DOI: 10.1124/mol.117.109199
This article has not been copyedited and formatted. The final version may differ from this version.

Raymond V and Sattelle DB (2002) Novel animal-health drug targets from ligand-gated chloride channels. *Nat Rev Drug Discov* **1**:427-436.

Schnizler K, Saeger B, Pfeffer C, Gerbaulet A, Ebbinghaus-Kintscher U, Methfessel C, Franken EM, Raming K, Wetzel CH, Saras A, Pusch H, Hatt H and Gisselmann G (2005) A novel chloride channel in *Drosophila melanogaster* is inhibited by protons. *J Biol Chem* **280**:16254-16262.

Shimomura M, Okuda H, Matsuda K, Komai K, Akamatsu M and Sattelle DB (2002) Effects of mutations of a glutamine residue in loop D of the α7 nicotinic acetylcholine receptor on agonist profiles for neonicotinoid insecticides and related ligands. *Br J Pharmacol* **137**:162-169.

Shimomura M, Yokota M, Ihara M, Akamatsu M, Sattelle DB and Matsuda K (2006) Role in the selectivity of neonicotinoids of insect-specific basic residues in loop D of the nicotinic acetylcholine receptor agonist binding site. *Mol Pharmacol* **70**:1255-1263.

Sine SM and Engel AG (2006) Recent advances in Cys-loop receptor structure and function. *Nature* **440**:448-455.

Sparks TC, Watson GB, Loso MR, Geng C, Babcock JM and Thomas JD (2013) Sulfoxaflor and the sulfoximine insecticides: chemistry, mode of action and basis for efficacy on resistant insects. *Pestic Biochem Physiol* **107**:1-7.

Thany SH, Lenaers G, Raymond-Delpech V, Sattelle DB and Lapied B (2007) Exploring the pharmacological properties of insect nicotinic acetylcholine receptors. *Trends Pharmacol Sci* **28**:14-22.

Tomizawa M and Casida JE (2003) Selective toxicity of neonicotinoids attributable to specificity of insect and mammalian nicotinic receptors. *Annu Rev Entomol* **48**:339-364.

Tomizawa M and Casida JE (2005) Neonicotinoid insecticide toxicology: mechanisms of selective action. *Annu Rev Pharmacol Toxicol* **45**:247-268.

Webb B and Sali A (2014) Comparative Protein Structure Modeling Using MODELLER. *Curr Protoc Bioinformatics* **47**:5 6 1-32.

Molecular Pharmacology Fast Forward. Published on July 24, 2017 as DOI: 10.1124/mol.117.109199
This article has not been copyedited and formatted. The final version may differ from this version.

Wolstenholme AJ (2012) Glutamate-gated chloride channels. *J Biol Chem* **287**:40232-40238.

Zhang W, Holyoke CW, Jr., Pahutski TF, Lahm GP, Barry JD, Cordova D, Leighty RM, Singh V, Vicent DR, Tong MT, Hughes KA, McCann SF, Henry YT, Xu M and Briddell TA (2017) Mesoionic pyrido[1,2-a]pyrimidinones: Discovery of triflumezopyrim as a potent hopper insecticide1. *Bioorg Med Chem Lett* **27**:16-20.

Zheng Y, Hirschberg B, Yuan J, Wang AP, Hunt DC, Ludmerer SW, Schmatz DM and Cully DF (2002) Identification of two novel *Drosophila melanogaster* histamine-gated chloride channel subunits expressed in the eye. *J Biol Chem* **277**:2000-2005.

Molecular Pharmacology Fast Forward. Published on July 24, 2017 as DOI: 10.1124/mol.117.109199
This article has not been copyedited and formatted. The final version may differ from this version.

Footnote

This study was supported by KAKENHI (Grant-in-Aid for Scientific Research (A)) from the Japan Society for the Promotion of Science [Grant 17H01472].

Molecular Pharmacology Fast Forward. Published on July 24, 2017 as DOI: 10.1124/mol.117.109199
This article has not been copyedited and formatted. The final version may differ from this version.

Figure legends

Figure 1. Genomic organization (A) and exon selection of variants of pHCl (B) expressed in the larvae of *Bombyx mori*. Variants 3, 9, 42 and 44 were expressed in all the tissues examined, and of these, variant 9 was expressed most abundantly. Variants 28–51 are presumed to be non-functional as chloride channels, since they lack TM1 and a part of TM2, due to omission of exon 11.

Figure 2. 2D clustering of *Bombyx* larvae tissues vs exon selection. When calculating the Z scores for the exon selection, data for exon 1 (E1), E2, E4, E5, E7, E8, E12 and E17ii were omitted because all of the transcripts contained these exons. The color bar represents exon selection frequency in which red and blue indicate high and low frequency, respectively. The results indicate a distinct exon selection within the T3G compared to the brain and midgut.

Molecular Pharmacology Fast Forward. Published on July 24, 2017 as DOI: 10.1124/mol.117.109199
This article has not been copyedited and formatted. The final version may differ from this version.

Figure 3. Characterization of *Bombyx* pHCl variant 9 expressed in *Xenopus laevis* oocytes using two-electrode voltage-clamp electrophysiological recording. (A) Inward currents induced in response to a shift in extracellular pH from 7.6 to 9.0. (B) Relationships between inward current amplitude in response to a pH shift from 7.6 to 9.0 and membrane potential at two different extracellular chloride concentrations. Each data plot is represented as the mean ± standard deviation of the mean (n = 3). (C) Inward currents induced in oocytes expressing variant 9 in response to extracellular pH shifts from 5.5 to a range of higher values. (D) Relationship between the normalized peak current amplitude of the response of variant 9 and extracellular pH. Each data point represents mean ± standard deviation of the mean (n = 4).

Molecular Pharmacology Fast Forward. Published on July 24, 2017 as DOI: 10.1124/mol.117.109199
This article has not been copyedited and formatted. The final version may differ from this version.

Figure 4. Actions of ivermectin on *Bombyx* pHCl variant 9 expressed in *Xenopus laevis* oocytes. (A) Inward currents induced by 10 μM ivermectin bath-applied extracellularly to oocytes expressing variant 9. Horizontal lines indicate the application of ivermectin. (B) Ivermectin concentration–response relationship determined at four different extracellular pHs. No substantial differences were observed in the EC_{50} for ivermectin at the pHs tested. Each data point represents mean ± standard deviation of the mean (n = 4).

Figure 5. Identification of the amino acid(s) underpinning differential ivermectin action on variants 1 and 9 of the *Bombyx* pHCl. (A) Amino acid sequence of variants 1 and 9. The different amino acids between variants 1 and 9 are boxed. (B) Responses of oocytes expressing wild-type and mutant variants 1 and 9 of *Bombyx* pHCl to 10 μM ivermectin at pH 8.5. Horizontal lines indicate the application of 10 μM ivermectin. (C) Comparison of peak current amplitude of the response to 10 μM ivermectin in oocytes expressing the two variants at pH 8.5. Each bar graph represents mean ± standard deviation of the mean (n = 5). An asterisk indicates that the difference of the two response amplitudes compared is significant by one-way ANOVA (Dunnett's test, $P < 0.05$).

Molecular Pharmacology Fast Forward. Published on July 24, 2017 as DOI: 10.1124/mol.117.109199
This article has not been copyedited and formatted. The final version may differ from this version.

Figure 6. Homology models of variants 1 and 9 of *Bombyx* pHCl. The models are illustrated as grey cartoon except for ivermectin, Val275 and Ser275 which are illustrated as spheres using PyMOL software. Carbons and oxygens of ivermectin are colored light blue and red, respectively, whereas carbons and oxygens of Val275 and Ser275 are colored yellow and red, respectively. (A) Side view of variant 9 with ivermectin bound at the allosteric site. Note that Ser275 is located at the channel gate that faces the cytoplasm. (B) Bottom view of variants 1 and 9. Both Val275 and Ser275 interact with Ala273. Since Ser275 is sterically smaller than Val275, it may permit more flexible movement of Ala273 in the chloride channel opening in response to ivermectin binding to the allosteric site.

Molecular Pharmacology Fast Forward. Published on July 24, 2017 as DOI: 10.1124/mol.117.109199
This article has not been copyedited and formatted. The final version may differ from this version.

Table 1. pEC_{50} values of ivermectin for variant 9 of *Bombyx* pHCl determined by fitting concentration curves at four different pHs.

	Extracellular pH			
	5.5	6.5	7.6	8.5
pEC_{50}	5.54 ± 0.03	5.53 ± 0.04	5.53 ± 0.04	5.56 ± 0.03

pEC_{50} (= -logEC_{50}) values are represented as the mean ± standard error of the mean (n = 4). No substantial differences were observed between the pEC_{50} values when analyzed using one-way ANOVA (Tuley's test).

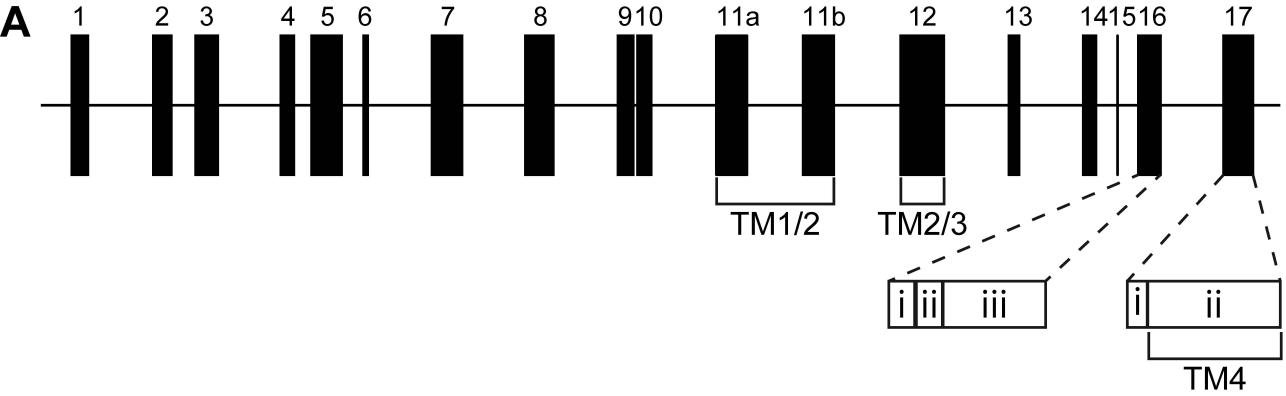

B

Expression
All Three Organs
Brain
T3G
Midgut
Brain and T3G
T3G and Midgut
Brain and Midgut

Variant numbers	Exon numbers																				Detection (%)
	1	2	3	4	5	6	7	8	9	10	11a	11b	12	13	14	15	16i	16ii	16iii	17i	17ii	
1																						0.67
2																						0.67
3																						6.7
4																						0.67
5																						0.67
6																						1.3
7																						0.67
8																						0.67
9																						8.0
10																						0.67
11																						1.3
12																						0.67
13																						1.3
14																						1.3
15																						0.67
16																						1.3
17																						0.67
18																						0.67
19																						0.67
20																						1.3
21																						0.67
22																						0.67
23																						0.67
24																						2.0
25																						1.3
26																						0.67
27																						0.67
28																						2.0
29																						1.3
30																						0.67
31																						0.67
32																						0.67
33																						0.67
34																						0.67
35																						0.67
36																						0.67
37																						2.0
38																						0.67
39																						0.67
40																						4.7
41																						0.67
42																						3.3
43																						1.3
44																						4.0
45																						0.67
46																						0.67
47																						0.67
48																						0.67
49																						0.67
50																						0.67
51																						0.67

Figure 1

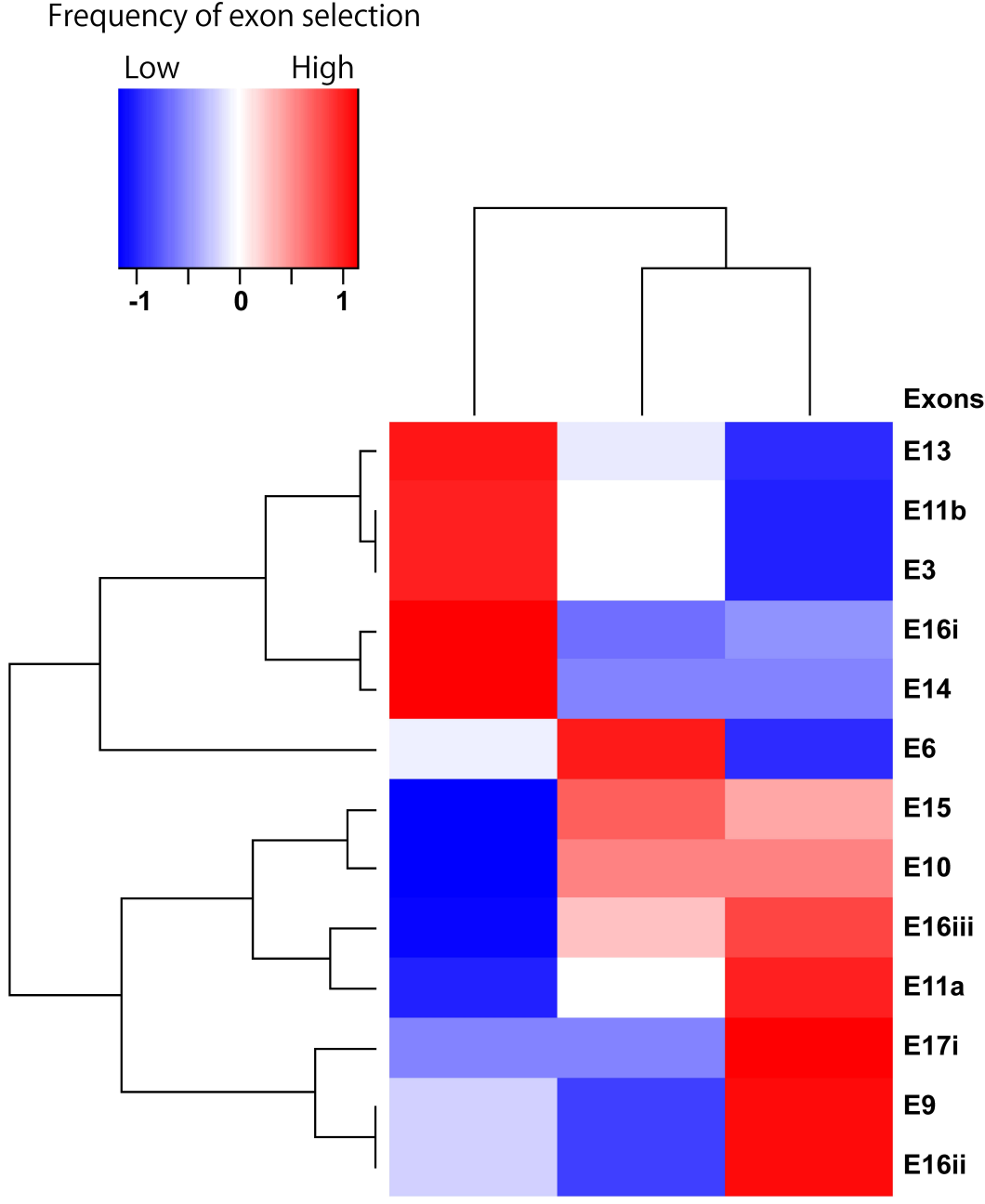
Frequency of exon selection
Low
High
-1
0
1
Exons
E13
E11b
E3
E16i
E14
E6
E15
E10
E16iii
E11a
E17i
E9
E16ii
Tissues
T3G
Midgut
Brain

Figure 2

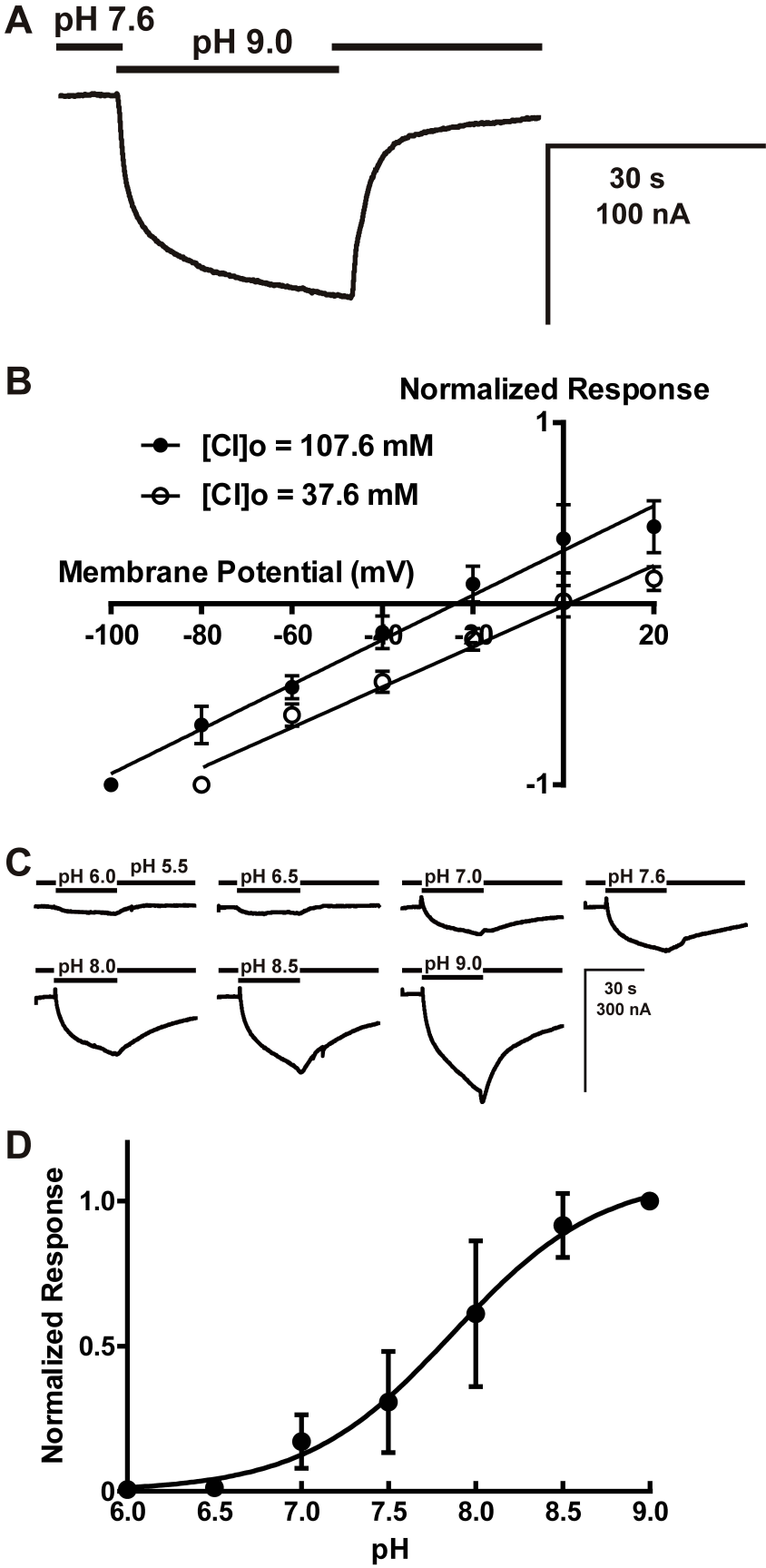
A
pH 7.6
pH 9.0
30 s
100 nA
B
Normalized Response
[Cl]o = 107.6 mM
[Cl]o = 37.6 mM
Membrane Potential (mV)
-100
-80
-60
-40
-20
20
1
-1
C
pH 6.0
pH 5.5
pH 6.5
pH 7.0
pH 7.6
pH 8.0
pH 8.5
pH 9.0
30 s
300 nA
D
Normalized Response
1.0
0.5
0
6.0
6.5
7.0
7.5
8.0
8.5
9.0
pH

Figure 3

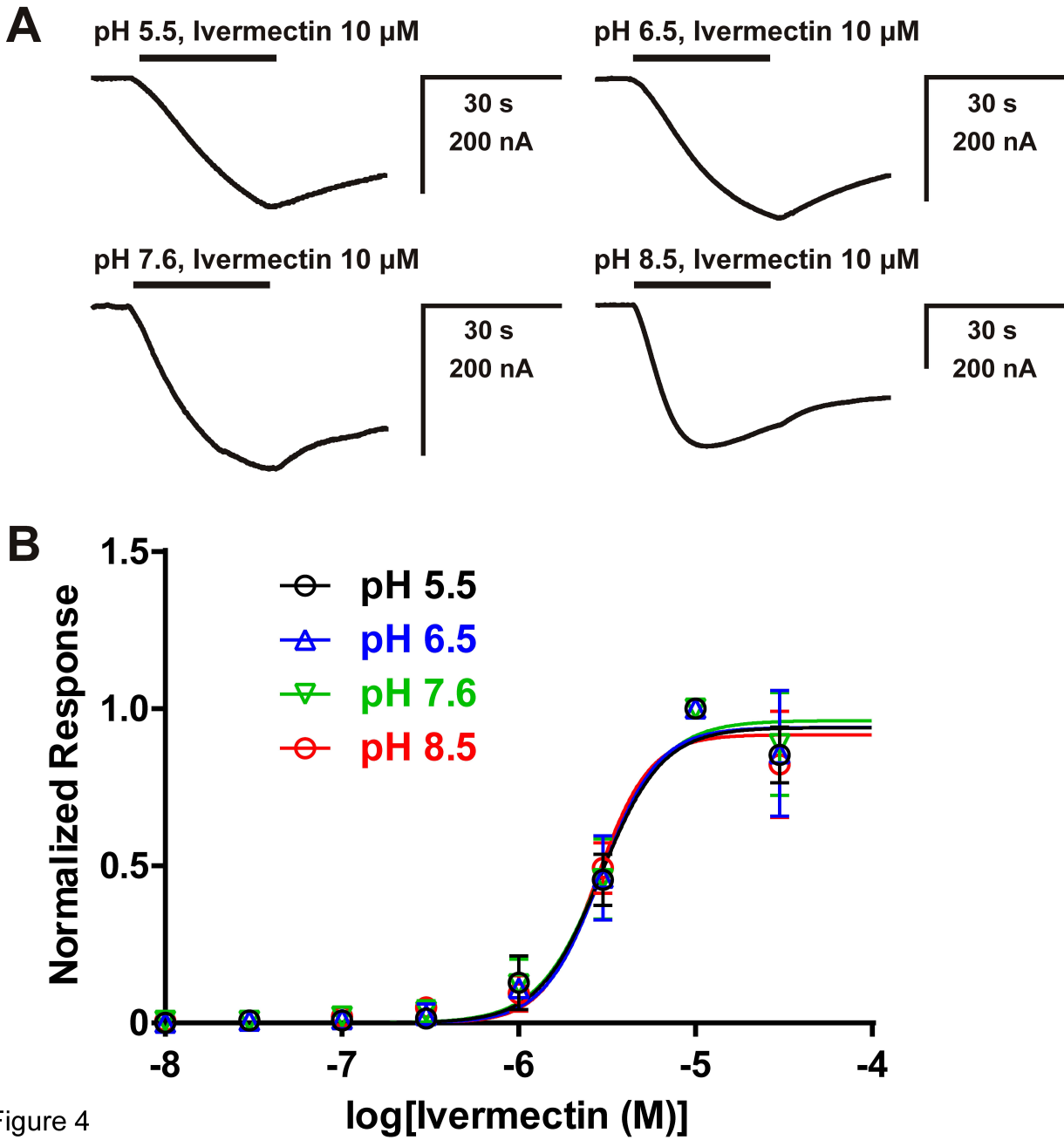
A
pH 5.5, Ivermectin 10 µM
30 s
200 nA
pH 6.5, Ivermectin 10 µM
30 s
200 nA
pH 7.6, Ivermectin 10 µM
30 s
200 nA
pH 8.5, Ivermectin 10 µM
30 s
200 nA
B
Normalized Response
1.5
1.0
0.5
0
pH 5.5
pH 6.5
pH 7.6
pH 8.5
-8
-7
-6
-5
-4
log[Ivermectin (M)]

Figure 4

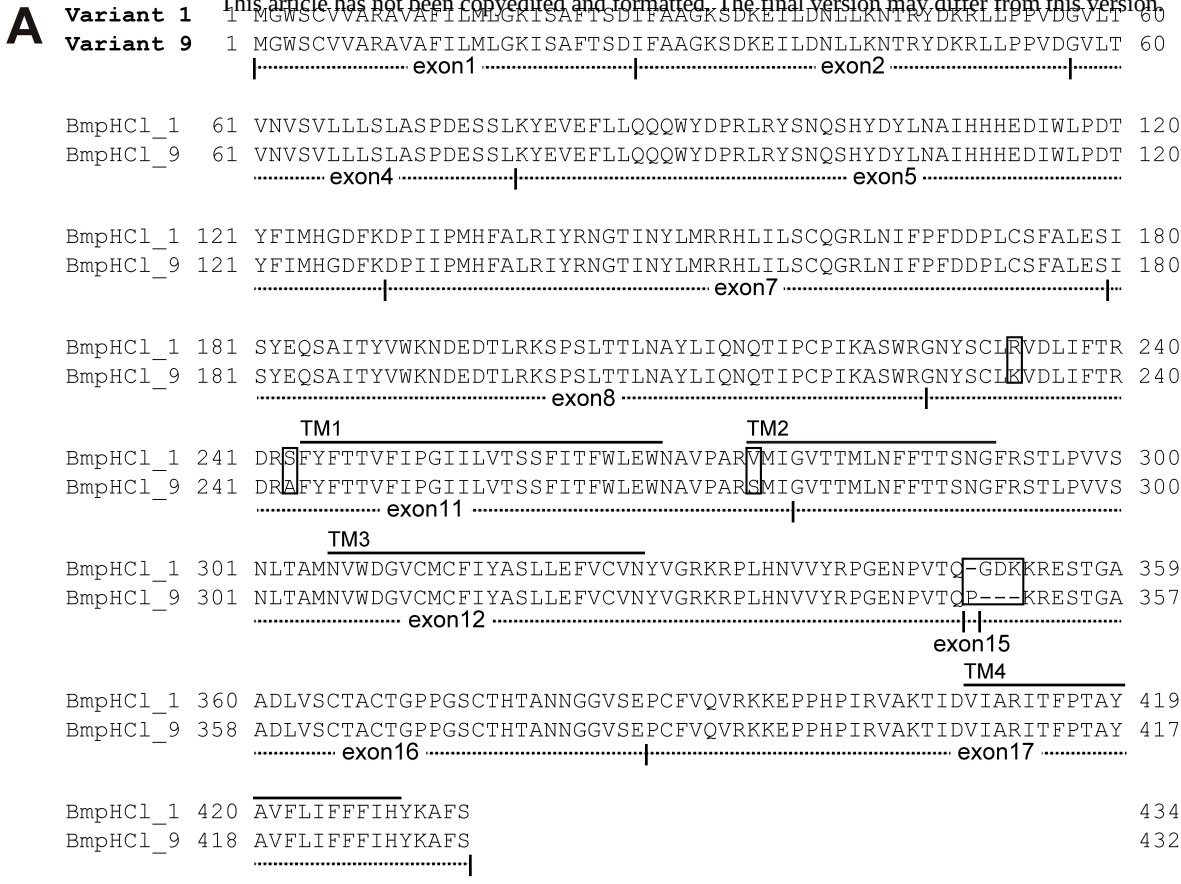

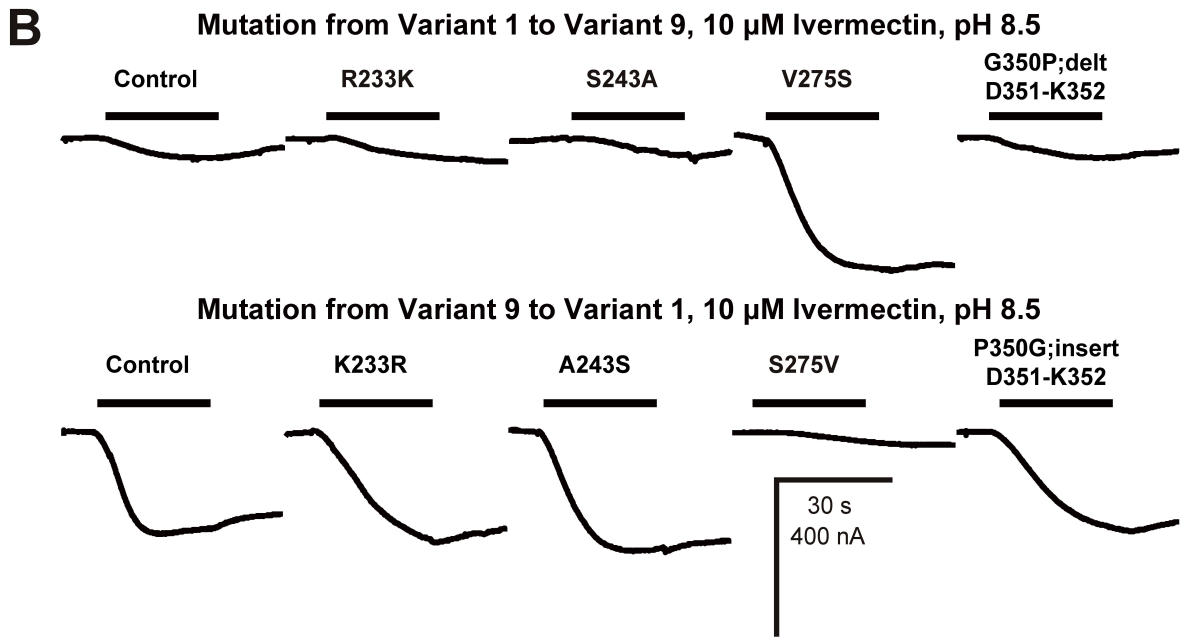

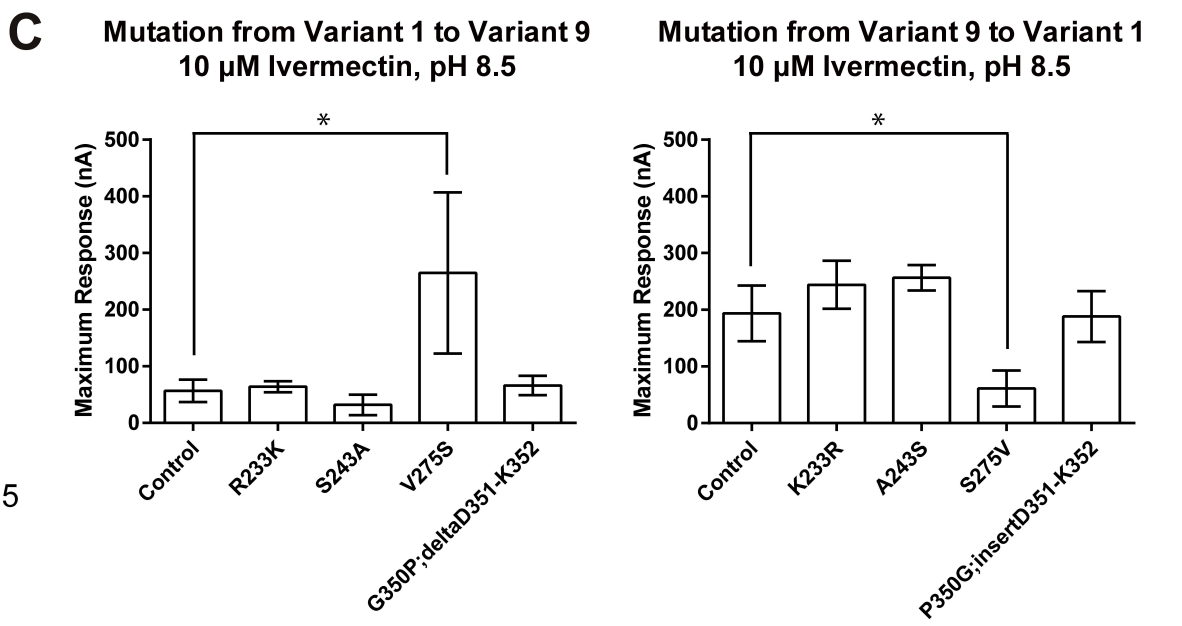

Figure 5

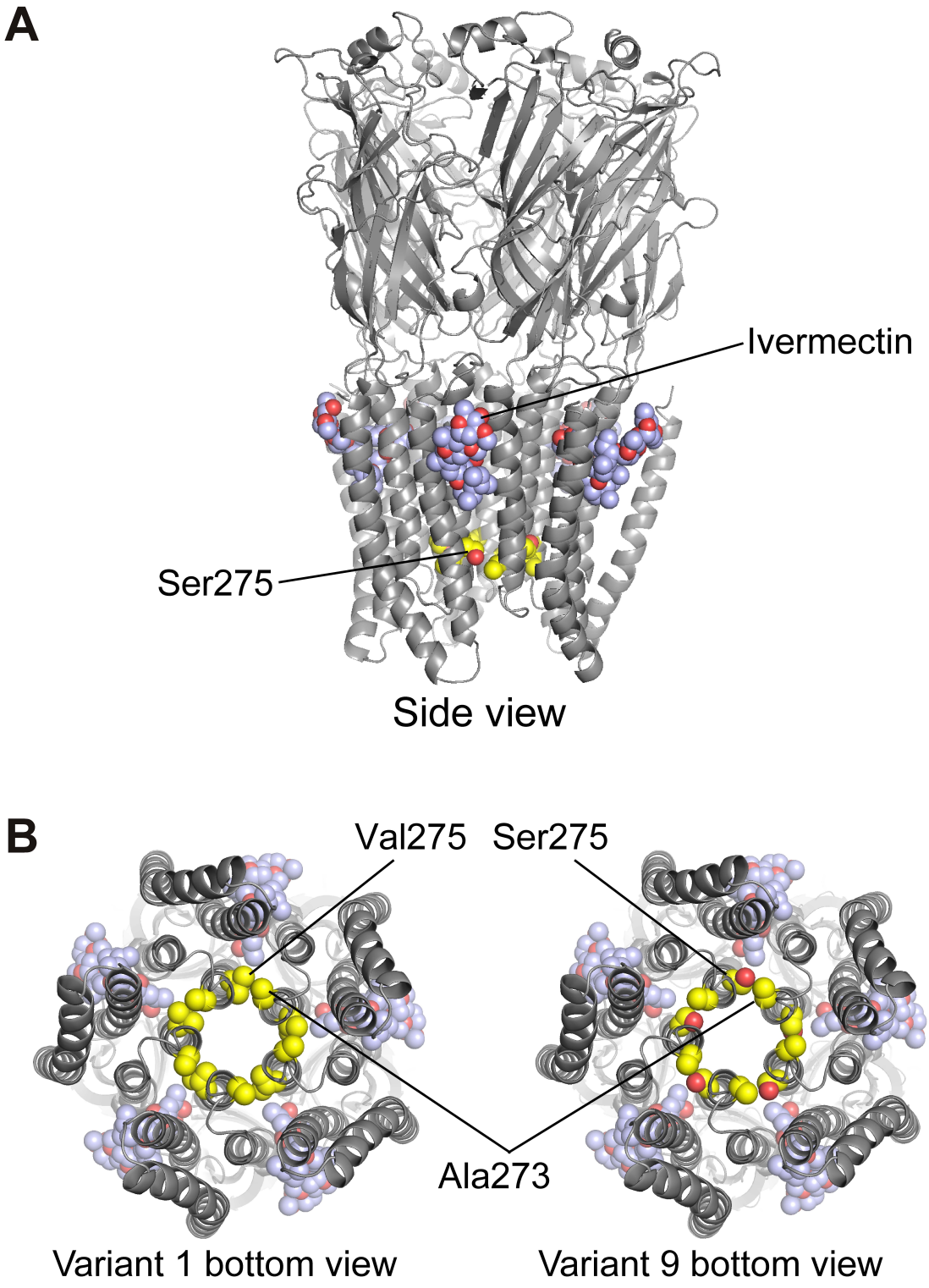
A
Ivermectin
Ser275
Side view
B
Val275
Ser275
Ala273
Variant 1 bottom view
Variant 9 bottom view

Figure 6